Modeling of Heavy-Oil Flow with Regard to Their Rheological Properties

Ilia Beloglazov [1], Valentin Morenov [2,*], Ekaterina Leusheva [2] and Ove T. Gudmestad [3]

1 Department of Mineral Processing, Saint Petersburg Mining University, 199106 Saint Petersburg, Russia; Beloglazov_II@pers.spmi.ru
2 Department of Oil and Gas, Saint Petersburg Mining University, 199106 Saint Petersburg, Russia; Leusheva_EL@pers.spmi.ru
3 Faculty of Science and Technology, University of Stavanger, N-4036 Stavanger, Norway; otgudmestad@gmail.com
* Correspondence: morenov@spmi.ru; Tel.: +7-812-328-8420

Abstract: With the depletion of traditional energy resources, the share of heavy-oil production has been increasing recently. According to some estimates, their reserves account for 80% of the world's oil resources. Costs for extraction of heavy oil and natural bitumen are 3–4 times higher than the costs of extracting light oil, which is due not only to higher density and viscosity indicators but also to insufficient development of equipment and technologies for the extraction, transportation, and processing of such oils. Currently, a single pipeline system is used to pump both light and heavy oil. Therefore, it is necessary to take into account the features of the heavy-oil pumping mode. This paper presents mathematical models of heavy-oil flow in oil-field pipelines. The rheological properties of several heavy-oil samples were determined by experiments. The dependencies obtained were used as input data for a simulation model using computational fluid dynamics (CFD) methods. The modeling condition investigates the range of shear rates up to 300 s^{-1}. At the same time, results up to 30 s^{-1} are considered in the developed computational models. The methodology of the research is, thus, based on a CFD approach with experimental confirmation of the results obtained. The proposed rheological flow model for heavy oil reflects the dynamics of the internal structural transformation during petroleum transportation. The validity of the model is confirmed by a comparison between the theoretical and the obtained experimental results. The results of the conducted research can be considered during the selection of heavy-oil treatment techniques for its efficient transportation.

Keywords: heavy oil; rheology; oil-field pipeline; flow model; ANSYS

1. Introduction

The depletion of conventional hydrocarbon reserves is creating a need to develop hard-to-recover oil deposits, such as heavy- and high-viscosity oils or, in general, heavy-oil blends (HOB). The reserves of these types of oils are more than two times the reserves of traditional oil [1]. As a rule, HOB is characterized by high viscosity and density, and increased content of various metals such as vanadium, nickel, gold, zinc, copper, etc. [2–4]. It is necessary to take into account these properties of HOB when assessing their possible hazardous influence on the environment [5]. Among the parameters describing the rheological properties of oil, in practice, parameters characterizing its structural properties are most often used [6,7].

Whereas production costs for heavy-oil extraction are usually higher than those for conventional oil, the introduction of enhanced oil-recovery techniques (e.g., steam-assisted gravity drainage, toe-to-heel air injection, etc.) leads to increased recovery rates and, consequently, to decreasing costs [8].

These methods are needed to provide for flowability and sustainable production of heavy oil. Thus, various treatment techniques aimed at effecting rheological properties of

high-viscosity or heavy oil are necessary for efficient production. Physical and chemical treatments considers several method to ensure efficient recovery of HOB [9]. The thermal effect is a common way to provide stable hydrocarbon production, especially when considering complicated climate conditions with low temperatures of ambient air, such as the Arctic region [10]. Many oil fields there are characterized by hard-to-recover reserves, such as heavy oil and high-viscosity oil. Another method of sustainable recovery is the application of pour point depressants and exposure of heavy hydrocarbons to ultrasonic fields, which can be considered more environmentally friendly than thermal methods [11].

Issues of heavy-oil flow simulation are especially important. Though the main concerns are extraction, production, and transportation, modeling techniques ensure successful development. Each stage of oil production has its own peculiarities concerning flow simulation; thus, it is necessary to consider a specific technological process individually. The lifting of well fluids from the borehole bottom to the wellhead presents quite a challenge for flow simulation. Possible changes in the mode of well operation, such as stops and start-ups of the pumps, lead to changes in rheological characteristics of the fluid and, consequently, flow regimes that pose a danger for stable and efficient production [12]. The specifics of non-Newtonian fluid flow simulations in annular medium, such as in the oil well, are needed to calculate possible changes in the pressure loss during transient processes, which should be noted during well operations or application of enhanced oil recovery techniques [13].

Although the problem of investigating the properties of non-Newtonian fluids and their behavior during flow in the wellbore was considered in some works [14,15], the proper calculation of the rheological characteristics of heavy oils and HOBs and their corresponding flow simulation models during lifting in the well is still a challenge.

For example, the Yaregskoye field produces unique heavy high-viscosity oil, from which a significant amount of valuable and high-quality oils products and bitumen can be obtained [16]. Heavy oil with a density of 964.4 kg/m^3 at 20 °C and a naphthenic-aromatic base is being produced at the Yaregskoye field. This oil is mixed with other oils from the northern fields of the Timan-Pechora oil and gas province and is transported further through the pipeline. Most of the oils from the northern fields are characterized by anomalous properties: high pour point and high viscosity. It should be noted that these indicators only increase every year (Table 1), worsening the transport performance of the pumped oils, which leads to an increase in both economic and technological costs during the construction and operation of equipment necessary for pumping such oils [17].

Table 1. Properties of oil blends pumped through the Timan-Pechora trunk pipeline in different periods of operation.

Parameter	1970–80	1980–90	1990–2000	2000–10	2010–20
Density at 20 °C, kg/m^3	833–838	870–875	860–865	860–865	860–865
Dynamic Viscosity at 0 °C, mPa·s	45–60	120–130	90–105	100–126	180–200
Paraffin content, % mass.	5–6	2.5–3.5	6–7	6–9	8–10
Temperature of the structure formation, °C	12–15	6–8	14–16	14–18	19–21
Pour point, °C	4–6	0–2	6–8	7–14	10–15

The Varandey sea terminal on the Pechora Sea coast in the Arctic was recently commissioned, specially designed to transport oil from the Timan-Pechora province. The northern route through the Barents Sea offers an alternative supply to both the European and American markets. It can be assumed that new opportunities will appear in the company's logistics plans for Yarega oil, where it will be mixed with paraffinic oil from the Varandey field [18].

Thus, the aim of this paper is to assess the physical, chemical, and specifically the rheological properties of heavy-oil blends and their influence on flow parameters during pumping through the oil-field pipelines. It should be noted that the oils under consideration are non-Newtonian anomalously viscous liquids, the interaction of which can cause a

deterioration in the flow characteristics of the blend obtained from them. In this regard, the question arises of finding optimal solutions for influencing the oil flow in order to improve the physical, chemical, structural, and mechanical properties of the heavy hydrocarbons. The results of the conducted research can be used for subsequent selection of the most effective solution to improve the transport characteristics of the oils. For example, one of the promising solutions is the treatment by ultrasound [19].

2. Materials and Methods

This work studied (as a case) the change in physical, chemical, and structural-mechanical properties (Table 2) for 4 blends of Yarega and Varandey oils with concentrations of heavy Yarega oil in blends at 10, 15, 25, and 50%.

Table 2. Physical, chemical, and structural-mechanical properties for 4 blends of Yarega and Varandey oils.

Blend	Kinematic Viscosity, mm^2/s	Pour Point, °C	Fractional Composition	
			Yield, % vol.	Fractioning Temperature, °C
Blend 1	7.874	+7	69	370
Blend 2	29.486	+9	60	359
Blend 3	11.921	+11	63	367
Blend 4	18.345	+15	57	349

A rotary viscometer Rheotest RN4.1 was used to conduct experiments in the study of the oil's rheological characteristics. Measurements were carried out in 0–600 rpm range of viscometer rotor speeds. Different rotation speeds of the rotational viscometer corresponded to different deformation rates of the fluid: from low speeds at the beginning of fluid motion to higher values during flow through the pipeline. Rheological parameters were determined using a viscoplastic and power-law solution model. A measuring system was necessary to study the rheological characteristics of substances with a viscosity of up to 100,000 mPa·s. It consisted of a stationary measuring cup and a cylindrical rotor, which was placed in this cup. To study the behavior of liquids at different temperatures, thermostat and thermo-insulated vessels were used [20].

2.1. Analytical Dependencies

In most cases, HOBs obey the law of a pseudoplastic fluid [21]. To describe the HOB motion, a theoretical rheological model is proposed:

$$\varepsilon = \varepsilon_f + \varepsilon_p + \varepsilon_n \tag{1}$$

where ε_f is frictional stress, ε_p is structural internal strength stress, and ε_n is dispersed flow viscosity stress.

Due to the thixotropy of the system, it can be assumed that ε_f and ε_p tend to zero with an increase in the velocity gradient and, therefore, will be described by an exponential dependence on the shear rate. When certain values of the velocity gradients are reached, HOBs move similarly to Newtonian fluid and its internal stresses is characterized only by viscous friction.

Frictional stress can be determined from the following equation:

$$\varepsilon_f = \delta_1 e^{-\tau\dot{\gamma}} \tag{2}$$

where δ_1 is the coefficient of frictional stress; τ is shear stress, Pa; and $\dot{\gamma}$ is the shear–strain rate (shear rate), s^{-1}.

If we consider a short time interval Δt, then it can be assumed that the relative decrease in the internal stress will be proportional to the shear gradient, whereas

$$\varepsilon_p = \delta_2 e^{-\Delta\tau\dot{\gamma}} \tag{3}$$

where δ_2 is the coefficient characterizing the internal strength of a structured flow.

For liquids similar to Newtonian ones, the dependence of shear stress on the velocity gradient [22] has the following form:

$$\varepsilon_n = \mu\dot{\gamma} \tag{4}$$

where μ is dynamic viscosity, Pa·s. Substituting Equations (2)–(4) into Equation (1), we obtain the following:

$$\varepsilon = \delta_1 e^{-\tau\dot{\gamma}} - \delta_2 e^{-\Delta\tau\dot{\gamma}} + \mu\dot{\gamma} \tag{5}$$

Equation (5) reflects the dynamics of internal structural transformations in HOBs and makes it possible to determine the shear stresses depending on the velocity gradients. As a result of the analytical calculation, a polynomial function was obtained [23]:

$$\varepsilon = 1912 e^{-0.597\dot{\gamma}} - 1905 e^{-0.603\dot{\gamma}} + 2.485\dot{\gamma} \tag{6}$$

2.2. Methods of Numerical Modeling

It is necessary to create a model that is adequate for the experimental data, which will further allow for investigations of ways to reduce pressure losses during oil production, e.g., by changing the velocity and mode of oil pumping or by changing the diameter of the pipeline.

There are many models implemented in various software for defining the non-Newtonian behavior of a fluid. The working medium investigated can be both a viscous Newtonian fluid and a non-Newtonian viscoplastic fluid, the behavior of which is described by one of the three most common rheological models [24,25]. The effective viscosity can take different forms depending on the rheology of the working medium. In most cases, HOBs obey the law of a pseudoplastic fluid [26]; therefore, a power-law model is used—the Ostwald–de Waele dependence:

$$\tau = \tau_y + K\dot{\gamma}^n \tag{7}$$

where τ_y is the yield stress at shear rate equal 0, K is the consistency index (a measure of the average viscosity of the fluid and proportional to the viscosity of the liquid), and n is the Power Law index (a measure of the deviation of the fluid from Newtonian). For $n = 1$, the liquid is Newtonian.

In the ANSYS software, the Ostwald–de Waele equation has the following form:

$$\mu = \mu_{ap} = K(\lambda\dot{\gamma})^{n-1} \tag{8}$$

where μ_{ap} is the apparent (dynamic) viscosity, Pa·s, and λ is the normalizing time constant. Here, a non-Newtonian is a fluid for which the shear stress is not linearly proportional to the shear–strain rate (shear rate). For such fluids, the apparent viscosity is the ratio of shear stress to shear rate for a given shear rate.

To represent the experimental dependence, the Ostwald–de Waele equation was chosen. The generalized reduced gradient (GRG) method, proposed by Lasdon et al. [27], was used for non-linear optimization [28]. The coefficients K, λ, and n were calculated so that there is minimum divergence with experimental data (Figure 1):

$$\mu = 12.848(0.7165\dot{\gamma})^{0.409-1} \tag{9}$$

If we simplify Equation (9) to the form $\mu = K\dot{\gamma}^{n-1}$, assuming $\lambda = 1$, then we can use a power-law approximation to fit the experimental function. As a result, the following equation was obtained:

$$\mu = 11.348\dot{\gamma}^{0.362-1} \tag{10}$$

The obtained approximation results describe the experimental function correctly. When setting the parameters for the Ostwald–de Waele model in ANSYS, both options (9)

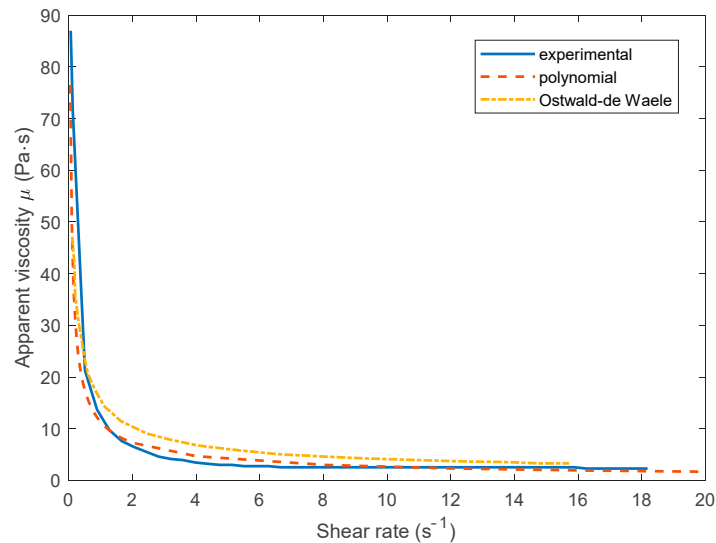and (10) are suitable, while the simplified form of the power approximation showed better convergence.

Figure 1. Approximation of the experimental viscosity curve and computational models.

Figure 2 shows how the oil viscosity decreases with increasing shear rate gradient, reaching its minimum value at a rate of about 6 s^{-1}. At higher values of the shear rate gradient, the oil under study can be considered a Newtonian fluid with a viscosity of 2.5 Pa·s.
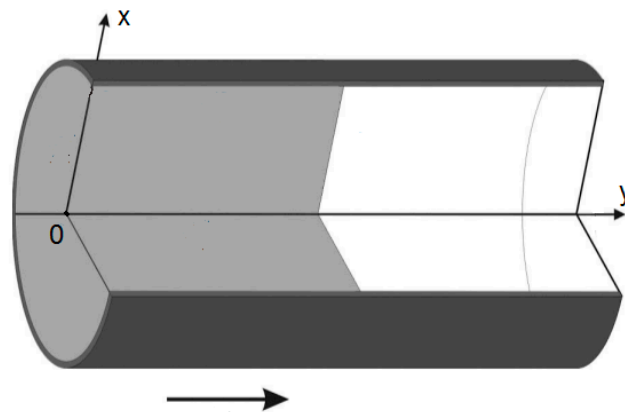

Figure 2. Statement of the solid modeling problem.

2.3. Mathematical and Numerical Modeling

The mathematical model of a non-Newtonian fluid flow processes is a set of Navier–Stokes equations in the stress tensor component form, the continuity equation, the rheological equation of the medium, and the boundary conditions set in a cylindrical coordinate system [29]. The equation of state for a non-Newtonian fluid is applicable to multiphase high-viscosity media, which, as mentioned above, is set in the form of an Ostwald–de Waele power law Equation (9) or a polynomial function Equation (6) as a custom expression.

The computational area is a section of an oil field pipeline designed to transport hydrocarbons from the wellhead to the treatment plant at the oil field. Often, these are pipelines with a diameter of up to 426 mm with an excess pressure of the medium up to 10 MPa. Under these conditions, the velocity of the HOB will be up to one meter per second.

To determine the hydrodynamic characteristics of the HOB influenced by the hydraulic resistance along the length of the pipeline and to compare the results for different HOBs

flowing under different conditions, a numerical model was created. Its creation included several stages.

At the first stage, the modeling area was built, which included the construction of solid geometry and the creation of a mesh in ANSYS. The considered scheme of fluid flow in the pipeline is shown in Figure 2. An axisymmetric section of the pipeline with an outer diameter of 299 mm and 3000 mm length was built in the CAD software.

The flow domain of the pipe was discretized using hexahedral elements oriented along the fluid flow for an axisymmetric channel (Figure 3). Mesh refinement in the wall region was also implemented.
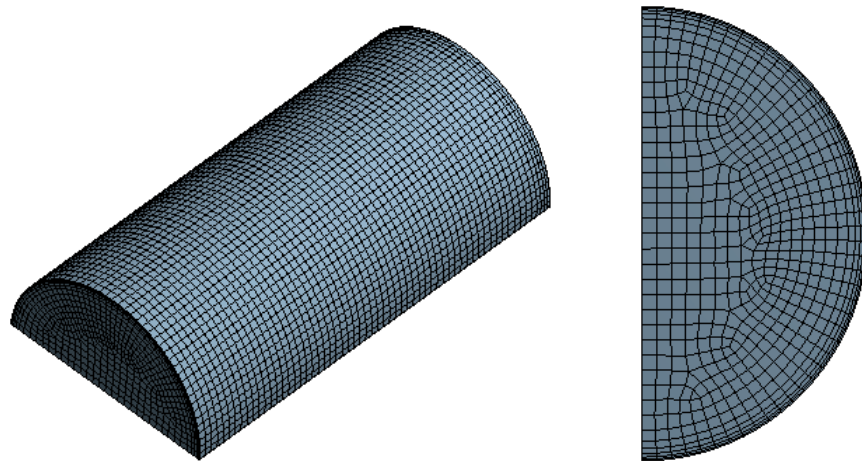

Figure 3. Computational mesh implementation: isometric and orthogonal view of the model.

The input data for the constructed model is given in the Table 3.

Table 3. Input data for the computational model.

Geometry Characteristics	
Inner cylinder dimeter, m	0.3
Length, m	3.0
Fluid Properties	
Fluid density, kg/m^3	945
Flow regime	laminar
Initial velocity, m/s	0.3–1.5

In turbulent flow, in most cases, values of shear rates are achieved that destroy the structure of the oil (for simulated oil—6 s^{-1}) and the viscosity becomes constant [30]. Therefore, when studying the non-Newtonian behavior of oil, the main interest is the laminar flow regime, in which low shear rates exist and the oil actively manifests its anomalous properties.

From a practical point of view, modeling the flow of oil in a laminar regime is justified by the fact that, during oil production, a turbulent flow regime is first achieved in the pipeline or submersible pump and that, during lifting and transportation, heavy oil has time to structure, a flow core is formed, and particles move with almost the same velocity in a laminar mode.

Below, we consider a fully developed stationary flow of an incompressible fluid in a laminar regime through a channel of constant cross section. The rheology of the working medium is described by a generalized Newtonian model. In this model, the medium is considered a nonlinear viscous fluid. The notion of the effective viscosity of the fluid, which

generally depends on the rate of the medium's deformation, is introduced in the model. In this formulation, the laminar flow regime is described by Navier–Stokes equations:

$$\nabla \cdot \left(\rho \vec{v} \right) = 0 \tag{11}$$

$$\rho \frac{d\vec{v}}{dt} + \nabla \cdot \left(\rho \vec{v} \vec{v} \right) = -\nabla p + \nabla \tau \tag{12}$$

where ρ is liquid density in kg/m^3; $\vec{v}$ is velocity vector; p is pressure, Pa; and ∇ is the Del (nabla) operator. For the generalized Newtonian model, the viscous stress tensor τ is determined as follows:

$$\tau = 2\mu S \tag{13}$$

where S is the strain rate tensor. The components of the strain rate tensor S have the following form:

$$S_{ij} = \frac{1}{2} \left(\frac{\partial u_i}{\partial x_j} + \frac{\partial u_j}{\partial x_i} \right) \tag{14}$$

The intensity of the strain rates for the medium is the second invariant of the strain rate tensor:

$$\dot{\gamma} = \sqrt{2SS} = \sqrt{2S_{ij}S_{ij}} \tag{15}$$

In (15), S_{ij} corresponds to gradients of mean velocity and mean shear rate, which together contribute to the shear rate tensor.

3. Results

Figure 4 shows the experimental dependencies of the shear stress τ in the HOB flow on shear rate $\dot{\gamma}$ at different temperatures.
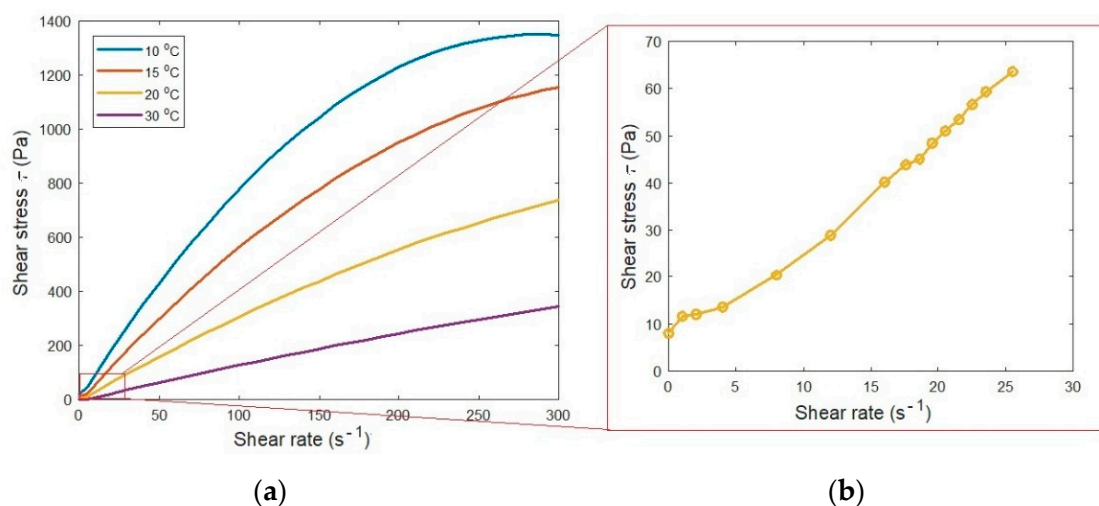

Figure 4. Rheogram of the fluid at different temperatures t (**a**) and magnified section of the rheogram at 20 °C (**b**).

Heavy oils are highly plastic nonlinear viscous non-Newtonian fluids, the rheological properties of which are described by the well-known Shvedov–Bingham equation [6]. However, in areas of low shear stresses, the dependence has a nonlinear form, which is not taken into account in the mentioned model. This region, which is difficult for modeling, is replaced by extrapolation of the straight-line part of the graph to zero shear rate, or other values of the parameters included in the Shvedov–Bingham model are calculated [7–9].

As an example, let us present the analytical (6) dependence of the shear stress on the shear rate for low values of shear rate obtained for the experimental characteristics of HOB flow at a temperature of 20 °C (see Figure 5).
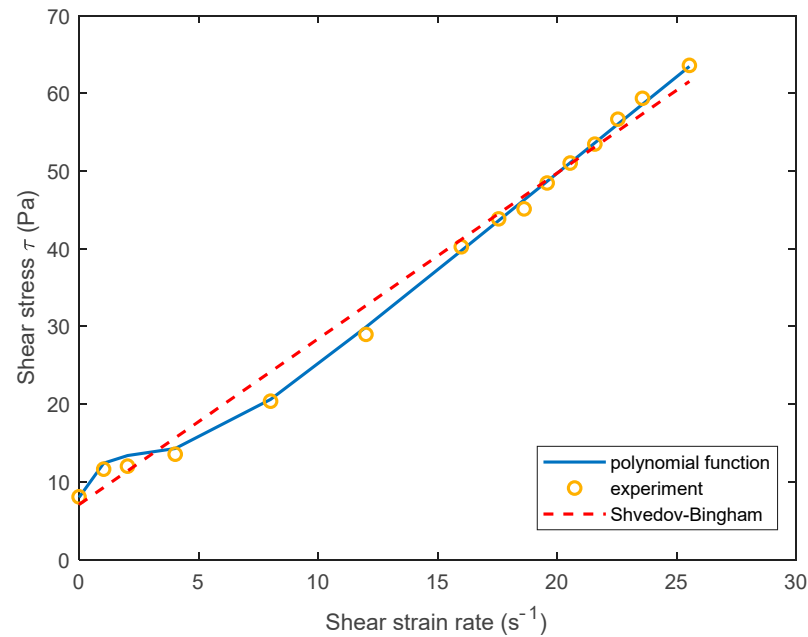
Figure 5. Experimental and analytical rheological dependencies of shear stress on shear rate.

Figure 5 shows that the experimental rheological data are in good agreement with the models in (6), (9) and (10) under the given boundary conditions when the initial fluid velocity is about 0.3–0.4 m/s.

The oil velocity values obtained in the simulation are plotted in Figure 6. The velocity profiles obtained from the simulations are shown in Figure 7. The presented profiles differ from the parabolic profiles of Newtonian fluid [31]. In particular, it should be noted that Figure 7 shows the velocity profiles for initial flow velocities of 1.5 and 1 m/s. These velocity profiles describe a mixed flow; however, calculations show that, even at high pressure gradients, a region of non-Newtonian flow remains near the center of the flow. In other words, during the flow of a non-Newtonian fluid with increasing velocity, the region of the non-Newtonian flow narrows, being localized to the center of the flow.
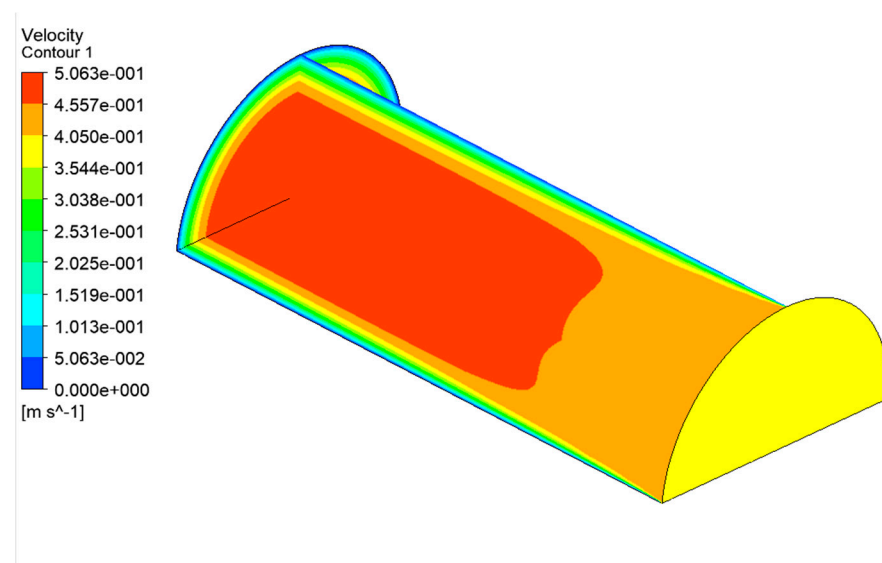

Figure 6. Simulated contours of the oil velocity distribution in the oil-field pipeline for an initial fluid flow velocity of 0.4 m/s.
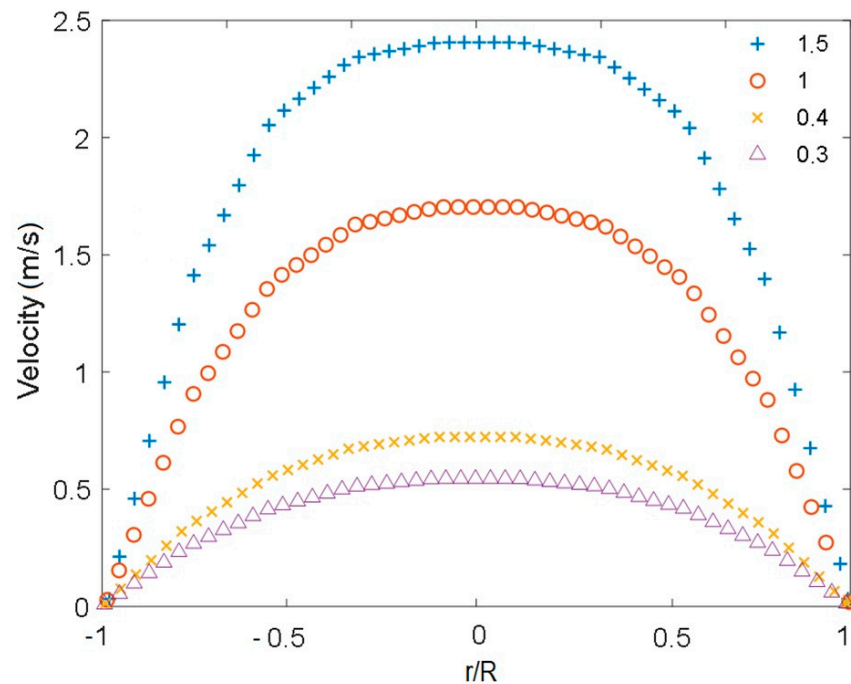
Figure 7. Simulated velocity profiles for different initial fluid flow velocities, where R is the pipe radius (m) and r is the radial location within the pipe (m).

Before evaluating the effect of oil viscosity on other parameters, one needs to make sure that the obtained results are correct by taking the viscosity curve from the simulation model and by comparing it with the curve obtained by substituting various values of the simulated shear rate $\dot{\gamma}$ in Equation (12), which, in turn, represents an approximation to experimental data.

At first glance, it can be assumed that the viscosity decreases towards the center of the pipeline, where the velocity (Figure 7) is higher, but in the case under consideration, the viscosity (Figure 8) is a function of one variable: the shear rate. Additionally, with an increase in the shear rate $\dot{\gamma}$, the viscosity μ decreases. However, the shear rate in the flow core is very low (Figure 9) even for the location with the highest velocity (Figure 6).
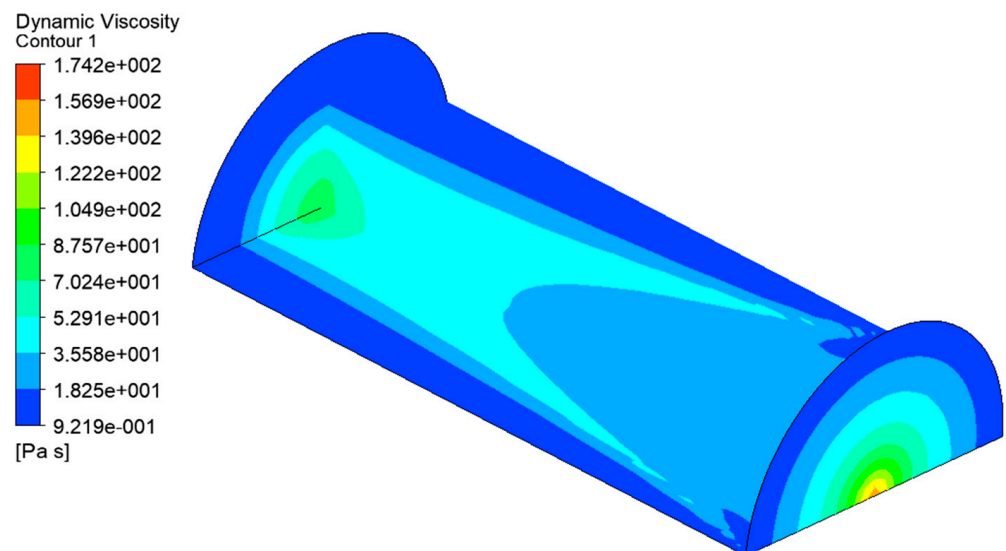

Figure 8. Simulated contours of oil viscosity distribution in the oil-field pipeline.
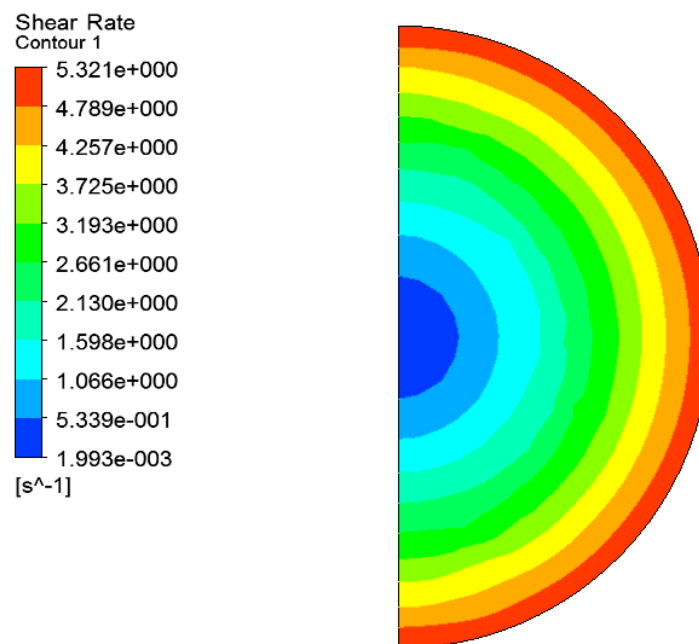
Figure 9. Simulated contours of shear rate between oil layers.

Another important characteristic to measure is the distribution of the pressure (Figure 10). Pressure drop per meter of the pipeline is calculated as the difference between the absolute pressure at the initial and ending points (Figure 11).
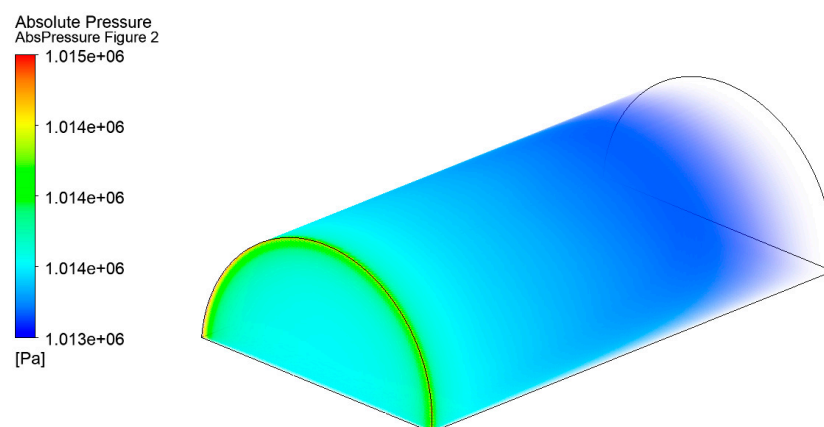

Figure 10. Simulated distribution of the absolute pressure in the pipeline.

The pressure drop (Figures 10 and 11) is almost linear. Figure 11 shows that, at the initial point of the pipeline, the pressure is about 1 MPa, which corresponds to the set 10 atm and an initial flow velocity of 0.4 m/s, and then the pressure gradually decreases. The exact pressure values at a distance from the pipeline inlet are illustrated by the differential pressure function in Figure 11 described by the following equation:

$$P_{abs} = -368.45 \cdot x + P_{in} \tag{16}$$

where P_{abs} is the absolute pressure after x meters from the pipeline inlet, Pa, and P_{in} is the absolute pressure at the pipeline inlet, Pa.

Thus, when the pressure drops by 1 atm, the oil will have moved about 275 m. A similar result is achieved under the condition of a laminar flow regime in combination with the non-Newtonian behavior of oil.
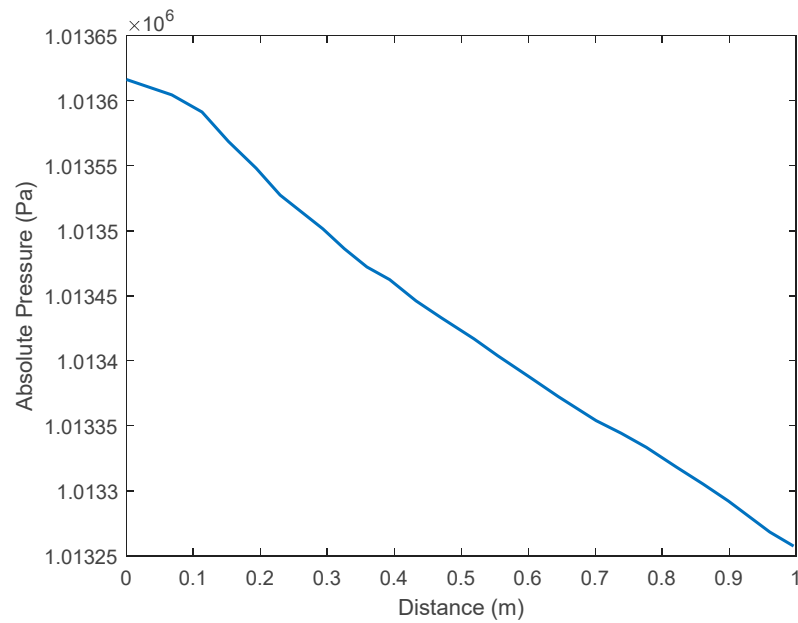
Figure 11. Pressure drop along the length of the pipeline.

Discrepancies between the experimental data and the values of viscosity obtained in the course of the modeling (Figure 12) are less noticeable; however, these discrepancies are associated with the approximation itself. The Ostwald–de Waele model is not optimal for describing the experimental data under consideration at low shear rates. However, it can be concluded that the calculated values of the viscosity in the course of the numerical simulation with a limited degree of error follows Equation (6), which was set to determine the viscosity. The best convergence in this simulation is provided by the model using the polynomial function (6).
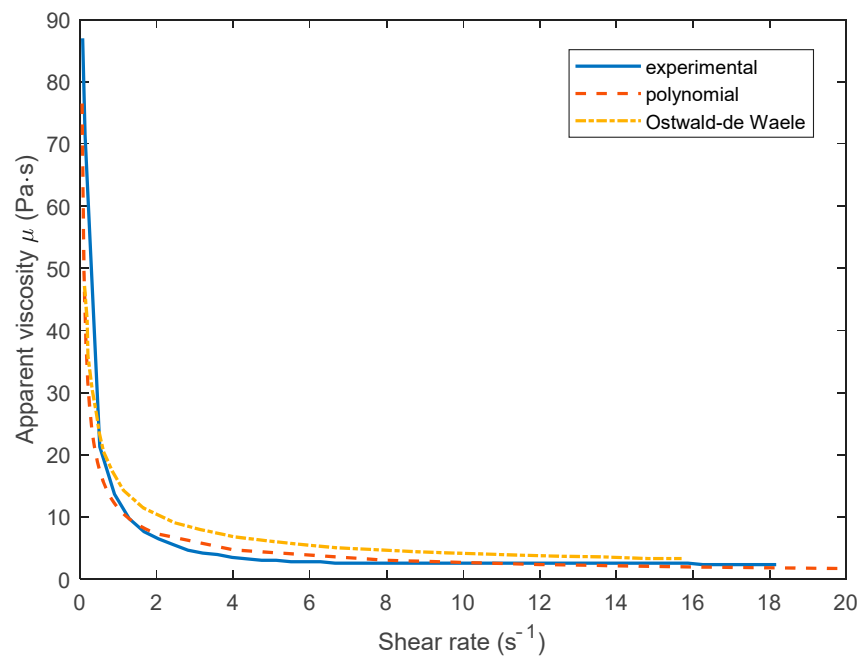

Figure 12. Comparison of the viscosity curve obtained during the simulation and the curve that approximates the experimental data.

The results obtained show that a refined model should be used for the dependence of shear stress on the velocity gradient in the form of an arbitrary function (6). This will bring the calculated values as close as possible to the experimental ones.

4. Discussion

The rheological equation of motion for heavy oil is theoretically substantiated, reflecting the dynamics of the internal structural transformations. A comparison of the calculated and experimental data confirms the validity of the proposed approach in modeling the rheological properties of heavy-oil flow.

Based on the analysis of the obtained data, several characteristic stages of changes in the structural properties of oil can be distinguished. At low shear rates (Figure 5), a structured layer of a certain strength is observed. As can be seen in the figure, the dependence has a nonlinear form, which is not taken into account in the existing equations for describing a non-Newtonian fluid (the Shvedov–Bingham equation). This difficult-to-model area is replaced by extrapolation of the straight-line part of the graph to zero shear rate, or other parameter values from the standard model are used [31,32].

With an increase in the shear rate, the friction forces gradually increase and the strength of the structured layer decreases, followed by its dispersion. At certain shear gradients, HOB transforms into a liquid–solid medium, which is a suspension of solid particles of paraffin and asphaltenes in light hydrocarbons, characterized by the Newtonian nature of motion.

Figure 12 shows how the oil viscosity decreases with increasing shear rate gradient, reaching a low value at a rate of about 6 s^{-1}. At values of shear rate above 30 s^{-1}, the oil studied, which is a typical very heavy oil, can be considered a Newtonian fluid with a viscosity of 2.5 Pa·s [1]. This behavior of the oil is explained by its structural features. Asphaltene micelles, stabilized by solvation layers consisting of aromatic, naphthenic hydrocarbons, and resins, form a flexible lattice under the action of the Van der Waals force. This lattice is destroyed when structured oil layers move relative to each other. As a result, the oil viscosity drops until the lattice is completely destroyed. To restore the bonds, the oil should be at a rest. This can be achieved not only by stopping production but also by moving it in a laminar mode, when adjacent oil layers have co-directional velocity vectors that do not differ much in magnitude. For these considerations, oil transportation is carried out in a turbulent mode [33,34].

The proposed modified rheological model has advantages in taking into account nonlinear components and can be used for drilling fluids at low shear rates. When considering drilling fluids in well circulation, where the velocity profile becomes flatter (Figure 7), the fluid velocity will be higher over a larger area of the annulus, which significantly improves the quality of wellbore cleaning. This is one of the reasons for non-Newtonian fluids with low Power Law indices providing such a high-quality wellbore cleaning.

The proposed model accurately describes the rheological properties of high-viscosity oils. The investigated range of kinematic viscosity was 7–30 mm^2/s, and the temperature range was 10–30 °C. Note that the studied ranges of temperature and viscosity correspond to the conditions of the oil-field transportation of heavy-oil blends. This allows for application of the developed model for simulation of flow pattern for oil blends with similar characteristics.

5. Conclusions

This study of oil viscosity shows that its structure, which determines its non-Newtonian behavior, is present until the shear rate gradient reaching a certain value at which the structure is destructed. The viscosity after destruction of the structure becomes constant. The simulation model developed reflects these principles, and most importantly, calculation of all values depending on viscosity is performed not with its averaged value but by using values acting at a given point.

For modeling the rheological properties of abnormally heavy oils in the investigated range of shear rate variation, Ostwald–de Waele models with various types of approximations can be efficiently used. However, in the region of low shear stresses (0–30 s^{-1}), the dependence will mostly be nonlinear, which is not taken into account in most known models. This difficult-to-model region can be described using a rheological model based on the approach proposed in this article by derivation of a polynomial function.

A laminar mode of oil flow has a high viscosity, and consequently, there is significant pressure drop as the shear rate gradient, sufficient for complete destruction of the structure, is achieved not only in the near-wall region but also in the core of the flow, where the bulk of the oil is transferred. The oil transportation must therefore, in this case, be in a turbulent mode.

On the basis of the simulation model developed, it is possible to test the effectiveness of various measures aimed at reducing pressure losses during oil transportation associated with its non-Newtonian characteristics.

Author Contributions: Conceptualization, I.B. and V.M.; formal analysis, E.L.; investigation, I.B.; methodology, V.M.; project administration, V.M. and E.L.; resources, V.M. and O.T.G.; software, I.B.; supervision, O.T.G.; validation, I.B.; visualization, E.L.; writing—original draft, I.B.; writing—review and editing, V.M. and O.T.G. All authors have read and agreed to the published version of the manuscript.

Institutional Review Board Statement: Not applicable.

Informed Consent Statement: Not applicable.

Data Availability Statement: The data presented in this study are available on request from the corresponding author. The data are not publicly available due to its storage in private networks.

Conflicts of Interest: The authors declare no conflict of interest.

Abbreviations

The following physical values are found in the article:

ε_f	frictional stress, Pa;
ε_p	structural internal strength stress, Pa;
ε_n	dispersed flow viscosity stress, Pa;
δ_1	coefficient of frictional stress;
δ_2	coefficient characterizing the internal strength of a structured flow;
τ	shear stress, Pa;
$\dot{\gamma}$	shear-strain rate (shear rate), s^{-1};
μ	dynamic viscosity, Pa·s;
μ_{ap}	apparent (dynamic) viscosity, Pa·s;
τ_y	yield stress at shear rate, equal 0;
K	consistency index;
n	Power Law index;
λ	normalizing time constant;
ρ	liquid density, kg/m^3;
$\overrightarrow{v}$	velocity vector;
p	pressure, Pa;
∇	Del (nabla) operator;
S	strain rate tensor;
P_{abs}	absolute pressure after x meters from the pipeline inlet, Pa;
P_{in}	absolute pressure at the pipeline inlet, Pa.

References

1. Litvinenko, V. The Role of Hydrocarbons in the Global Energy Agenda: The Focus on Liquefied Natural Gas. *Resources* **2020**, *9*, 59. [CrossRef]
2. Aleksandrova, T.; Aleksandrov, A.; Nikolaeva, N. An Investigation of the Possibility of Extraction of Metals from Heavy Oil. In *Mineral Processing and Extractive Metallurgy Review*; Taylor and Francis Inc.: Abingdon, UK, 2017; pp. 92–95. [CrossRef]
3. Issa, B.; Bazhin, V.Y.; Aleksandrova, T.A.; Povarov, V.G. Assessment of possibility of obtaining alloying components in the process of desalting of heavy hydrocarbon raw materials. Part 1. *CIS Iron Steel Rev.* **2020**, *19*, 8–12. [CrossRef]
4. Yakubov, M.R.; Milordov, D.V.; Yakubova, S.G.; Borisov, D.N.; Mironov, N.A. Resources and opportunities of vanadium and nickel concentration in field conditions during heavy oil partial upgrading processes before transportation. *Neftyanoe Khozyaystvo Oil Ind.* **2015**, *12*, 132–135.
5. Alekseenko, V.A.; Pashkevich, M.A.; Alekseenko, A.V. Metallisation and environmental management of mining site soils. *J. Geochem. Explor.* **2017**, *174*, 121–127.
6. Magomedov, R.N.; Popova, A.Z.; Maryutina, T.A.; Kadiev, K.M.; Khadzhiev, S.N. Current status and prospects of demetallization of heavy petroleum feedstock (Review). *Pet. Chem.* **2015**, *55*, 423–443. [CrossRef]
7. Manzhai, V.N.; Clovis Le Grand, M.M.; Terre, D.A. Rheological properties of heavy high-viscosity oil from Yaregskoye oil field. *Zap. Gorn. Inst.* **2012**, *195*, 73–77.
8. Ilinova, A.; Chanysheva, A. Algorithm for assessing the prospects of offshore oil and gas projects in the Arctic. *Energy Rep.* **2020**, *6*. [CrossRef]
9. Litvinenko, V.S.; Tsvetkov, P.S.; Dvoynikov, M.V.; Buslaev, G.V. Barriers to implementation of hydrogen initiatives in the context of global energy sustainable development. *J. Min. Instagram* **2020**, *244*, 421. [CrossRef]
10. Du, X.; Liu, J.; Liu, C. Study on Dynamic Simulation for Produced Oil-gas-water Mixtures Treatment Process in Offshore Heavy Oil Thermal Recovery. In Proceedings of the International Offshore and Polar Engineering Conference, Sapporo, Japan, 10–15 June 2018; pp. 48–51.
11. Kadyirov, A.; Karaeva, J. Ultrasonic and Heat Treatment of Crude Oils. *Energies* **2019**, *12*, 3084. [CrossRef]
12. Conde, J.; Banks, M. Producing heavy oil—The subsea brownfield challenge. In Proceedings of the Society of Petroleum Engineers—Abu Dhabi International Petroleum Exhibition and Conference, Abu Dhabi, UAE, 12–15 November 2018.
13. Ershadnia, R.; Amooie, M.A.; Shams, R.; Hajirezaie, S.; Liu, Y.; Jamshidi, S.; Soltanian, M.R. Non-Newtonian fluid flow dynamics in rotating annular media: Physics-based and data-driven modeling. *J. Pet. Sci. Eng.* **2020**, *185*, 106641. [CrossRef]
14. Dmitriev, M.S.; Ponomarenko, A.G.; Klachkov, A.P. Thermophysical Validation of the Technology of Asphalt-Resin-Paraffin Deposit Removal from Well Casings in Continuous High-Viscosity Oil Production Conditions. *Chem. Pet. Eng.* **2019**, *55*, 627–631. [CrossRef]
15. Kim, K.; Choi, H. Direct numerical simulation of a turbulent core-annular flow with water-lubricated high viscosity oil in a vertical pipe. *J. Fluid Mech.* **2018**, *849*, 419–447. [CrossRef]
16. Boytsova, A.A.; Kondrasheva, N.K.; Ancheyta, J. Pyrolysis Kinetics of Heavy Oil Asphaltenes under Steam Atmosphere at Different Pressures. *Energy Fuels* **2018**, *32*. [CrossRef]
17. Kondrasheva, N.K.; Baitalov, F.; Boitsova, A. Comparative assessment of structural-mechanical properties of heavy oils of Timano-Pechorskaya Province. *J. Min. Instgram* **2017**, *225*, 320–329. [CrossRef]
18. Stratiev, D.; Shishkova, I.; Tsaneva, T.; Mitkova, M.; Yordanov, D. Investigation of relations between properties of vacuum residual oils from different origin, and of their deasphalted and asphaltene fractions. *Fuel* **2016**, *170*, 115–129. [CrossRef]
19. Kozachok, M.V.; Krapivskiy, E.I.; Nekuchaev, V.O. Influence by physical flap on rheological characteristic transported heavy of the oils. In Proceedings of the 4th International Conference and Exhibition: New Discoveries through Integration of Geosciences, Saint Petersburg, Russia, 4 May 2010; European Association of Geoscientists and Engineers, EAGE: Moscow, Russia, 2010; p. cp-156-00196. [CrossRef]
20. ISO 3104:2020(en). Petroleum Products—Transparent and Opaque Liquids—Determination of Kinematic Viscosity and Calculation of Dynamic Viscosity. Available online: https://www.iso.org/standard/67965.html (accessed on 31 August 2020).
21. Nouar, C.; Frigaard, I.A. Non-linear stability of Poiseuille flow of a Bingham fluid: Theoretical results and comparison with phenomenological criteria. *J. Non Newton. Fluid Mech.* **2001**, *100*, 127–149. [CrossRef]
22. Draad, A.A.; Kuiken, G.D.C.; Nieuwstadt, F.T.M. Laminar-turbulent transition in pipe flow for Newtonian and non-Newtonian fluids. *J. Fluid Mech.* **1996**, *377*, 267–312. [CrossRef]
23. Aleksandrov, A.; Aleksandrova, T.; Romashev, A. Modeling of motion of heavy oil suspensions with regard to rheological properties of liquid in a circular pipe. In *International Multidisciplinary Scientific GeoConference Surveying Geology and Mining Ecology Management, SGEM*; International Multidisciplinary Scientific Geoconference: Albena, Bulgaria, 2017; pp. 729–734. [CrossRef]
24. Escudier, M.P.; Gouldson, I.W.; Pereira, A.S.; Pinho, F.T.; Poole, R.J. On the reproducibility of the rheology of shear-thinning liquids. *J. Non-Newton. Fluid Mech.* **2001**, *97*, 99–124. [CrossRef]
25. Barnes, H.A.; Hutton, J.F.; Walters, K. *An Introduction to Rheology*; Elsevier: Amsterdam, The Netherlands, 1989.
26. Chhabra, R.P.; Richardson, J.F. Non-Newtonian flow and applied rheology. In *Flow of Shear-Thinning Fluids in a Concentric Annulus*, 2nd ed.; Escudier, M.P., Gouldson, I.W., Eds.; Butterworth-Heineman: Oxford, UK, 2008.
27. Lasdon, L.S.; Waren, A.D.; Jain, A.; Ratner, M. Design and Testing of a Generalized Relaxed Gradient Code for Nonlinear Programming. *ACM Trans. Math. Soft.* **1978**, *4*, 34–50. [CrossRef]

28. Steven, C.C.; Raymond, P.C. *Numerical Methods for Engineers*; McGraw-Hill Higher Education: Boston, MA, USA, 2010.
29. Escudier, M.P.; Gouldson, I.W.; Jones, D.M. Flow of shear-thinning fluids in a concentric annulus. *Exp. Fluids* **1995**, *18*, 225–238. [CrossRef]
30. Tashbulatov, R.; Karimov, R.; Valeev, A.; Mastobaev, B. Modeling rheological properties of thixotropic oils at direct measurements on a rotary viscometer for evaluating the start-up modes of the trunk oil pipeline. *Neftyanoe Khozyaystvo Oil Ind.* **2020**, *4*, 80–84. [CrossRef]
31. Cross, M.M. Rheology of non-Newtonian fluids- A new flow equation for pseudoplastic systems. *J. Colloid. Sci.* **1965**, *20*, 417–437. [CrossRef]
32. Daly, B.J.; Harlow, F.H. Transport equations in turbulence. *Phys. Fluids* **1970**, *13*, 2634–2649. [CrossRef]
33. Radmir, T.; Rinat, K.; Anvar, V.; Alexander, K.; Boris, M. Modeling rheological properties in blending of anomalously viscous oils. *J. Eng. Appl. Sci.* **2018**, *13*, 4728–4732. [CrossRef]
34. Ancheyta, J. *Modeling of Processes and Reactors for Upgrading of Heavy Petroleum, Modeling of Processes and Reactors for Upgrading of Heavy Petroleum*; CRC: Boca Raton, FL, USA, 2013. [CrossRef]